JOC The Journal of Organic Chemistry

Article

pubs.acs.org/joc

From Phenyl Chlorides to α,n-Didehydrotoluenes via Phenyl Cations. A CPCM−CASMP2 Investigation

Davide Ravelli, Stefano Protti, Maurizio Fagnoni,* and Angelo Albini

PhotoGreen Lab, Department of Chemistry, University of Pavia, Viale Taramelli 12, 27100 Pavia, Italy

Supporting Information

ABSTRACT: Calculations with the complete active space self-consistent field (CASSCF) method were carried out for rationalizing the photochemical generation of the three isomeric didehydrotoluenes (DHTs) from the corresponding (*n*-chlorobenzyl)trimethylsilanes. Moreover, the original CASSCF energies were corrected through the introduction of the dynamic electron correlation term (at the MP2 level) and of an appropriate solvent model (CPCM). The work demonstrated the viability of intersystem crossing (conical intersection located) leading to the lowest lying triplet state of the silanes that fragments to give the corresponding triplet phenyl cations. The *para*- and *ortho*-isomers desilylate directly from such states of radical/radical cation character and yield the corresponding DHTs in their triplet state. Different from the other isomers, the *meta*-cation has a radical/radical cation structure in both spin states and thus two potential accesses to the different spin states of the corresponding DHT.

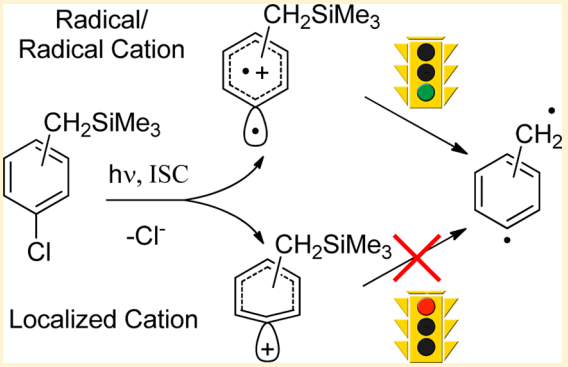

INTRODUCTION

The discovery that phenyl cations are conveniently generated from phenyl halides and esters by irradiation in polar media opened the access to a range of valuable applications. The chemistry occurring is spin dependent.[1−3] In the parent compound, the singlet is a localized cation of $\pi^6\sigma^0$ electronic configuration (Figure 1) that reacts unselectively so that the end result is solvolysis.[2] On the contrary, in the triplet state the two unpaired electrons are located in orthogonal spaces, the σ orbital at the dicoordinated carbon and a delocalized π orbital ($\pi^5\sigma^1$ structure, Figure 1). This intermediate undergoes homolytic hydrogen abstraction from the solvent or addition onto π-bond nucleophiles (Nu-H).[2,3]

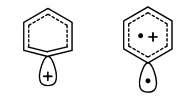

Figure 1. Lewis structures for the singlet (left, $\pi^6\sigma^0$ electronic structure) and triplet (right, $\pi^5\sigma^1$ electronic structure) states of parent phenyl cation.

The thermal generation of phenyl cations usually requires harsh conditions,[4] where the singlet is the only spin state accessible. On the other hand, triplet phenyl cations are smoothly generated upon photochemical heterolytic cleavage of aryl−halogen or aryl−oxygen bond in electron-rich aryl halides or esters (sulfonates or phosphates), respectively.[2,3] Thus, absorption of a photon allows for the population of the first excited state (S_1) of the aromatic precursor. Then, intersystem crossing (ISC) occurs, populating the lowest lying triplet state (T_1) from which heterolytic cleavage is feasible, thus generating the corresponding phenyl cation in the same multiplicity. A further ISC from the triplet cation to the corresponding singlet state is possible when the latter one is lower in energy.[1d,e]

Triplet phenyl cations may give access to further high energy intermediates.[5] In particular, we recently reported that these offered an alternative entry to α,*n*-didehydrotoluenes (DHTs).[6] The last species are heterosymmetric diradicals able to cleave single-stranded DNA[7] and thus claimed as potential chemotherapeutic agents. The generation in solution of such intermediates has been limited so far to the Myers−Saito cyclization of enyne−allenes, which applies only to the α,3-isomer.[8,9] In our approach, the irradiation of chlorobenzylsilanes **1a−c** generated triplet phenyl cations (^{3}**2$^+$a−c**) by heterolytic cleavage of the Ar−Cl bond and detachment of the trimethylsilyl cation (TMS^+) ensued to give α,*n*-didehydrotoluenes (**3a−c**), as depicted in Scheme 1. The presence of the $-CH_2TMS$ group had the 2-fold role of acting as an electron-donating moiety (comparable to −OMe, thus further facilitating the first cleavage)[10] and of bearing the electrofugal TMS cation.[11] In this way, all of the isomeric DHTs were formed.

To have a better insight into the double elimination occurring, we decided to carry out a computational analysis aimed at rationalizing the entire path leading from the aromatic precursors to DHTs, passing through the phenyl cation intermediates. A multireference method was required in order

Received: February 5, 2013
Published: March 11, 2013

   dx.doi.org/10.1021/jo400269s | J. Org. Chem. 2013, 78, 3814−3820

Scheme 1. Phenyl Cation-Mediated Strategy for the Photogeneration of α,*n*-Didehydrotoluenes

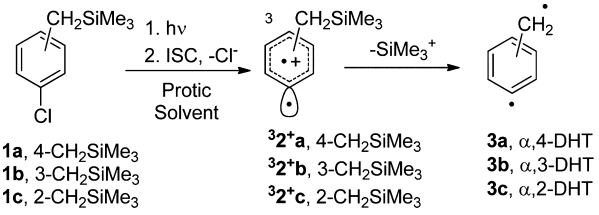

to describe correctly the electronic structure both of phenyl cations, as previously reported for singlet 4-aminophenyl cation,[12] and of diradical structures, such as DHTs.[13] Thus, we decided to use the complete active space self-consistent field (CASSCF) level of theory[14] to optimize the stationary points on the potential energy surfaces (PESs) of the species involved, as detailed below. CASSCF is considered one of the elective methods to handle excited states and further allowed to explore the whole path, from the excited states of the precursor to DHT. Thus, the singlet excited states ^{1}**1a**−**c** have been optimized and fully characterized, and the conical intersection (CoIn), expected to allow the ISC process between ^{1}**1a**−**c** and ^{3}**1a**−**c** has been located in **1a**, taken as a model. Moreover, corrections based on the second-order Møller−Plesset perturbation theory (MP2) have been applied to the original CASSCF energies (hereafter tagged as CASMP2), in order to obtain more reliable values thanks to the introduction of the dynamic electron correlation term.[15]

Computational Details. All of the calculations were carried out using the Gaussian 03[16] program package. In our investigation, the level of theory chosen for the optimization of all of the stationary points was CASSCF by using the standard 6-31G(d) basis set. This is a multiconfiguration method (MCSCF), which makes use of all the configurations involving a set of molecular orbitals (MOs, the so-called "active space") and a given number of electrons. Thus, this set of configurations is indicated as CASSCF(n,m), where n is the number of electrons and m is the number of MOs of the active space (both occupied and virtual).

No symmetry constraint was applied to the structures investigated. Frequency calculations were performed in vacuo to check that energy minima had no imaginary frequencies. Further notice that numerical frequency calculations (FREQ = NUMER) have been adopted for **1a**−**c** and **2**$^+$**a**−**c** in order to curtail the amount of memory required for the calculation. The occupancies of the orbitals included in the active space were carefully checked, and the values observed were always higher than 0.01 and lower than 1.99 for all of the stationary points reported, as recommended. The investigation of conical intersection(s)[17] from the singlet excited state in **1a** was carried out in vacuo at the CASSCF/6-31G(d) level of theory via the OPT = CONICAL keyword and using the CASSCF = SLATERDET option in order to include the possibility of locating crossing points between states of different spin (see the Supporting Information for details).

Solvent effect was included by single-point calculations at the CPCM-CASSCF/6-31G(d) method (MeOH bulk) on the optimized geometries obtained in vacuo.[18] The solvent cavity was calculated using the united atom topological model applied on radii optimized for the HF/6-31G(d) level of theory (RADII = UAHF option). Atomic charges have been calculated in solvent bulk according to the Merz−Singh−Kollman scheme,[19] via the POP = MK keyword and have been labeled in the text as "q_{ESP}".

MP2 corrections have been calculated by single-point calculations at the CASSCF-MP2/6-31G(d) level on the optimized geometries obtained in vacuo, adopting a configuration threshold equal to 0.05 via the IOP (5/52 = 20) option. The CASMP2/6-31G(d) Gibbs free energies reported in the text (see Tables S1, S3, and S5 in the Supporting Information) have thus been calculated by means of eq 1 reported in the following

$$G_{CASMP2} = E_{0(CASSCF,CPCM)} + \Delta E_{CORR(MP2,vacuo)} + \Delta G_{CORR(CASSCF,vacuo)} \quad (1)$$

where $E_{0(CASSCF,CPCM)}$ is the total electronic energy calculated at the CPCM−CASSCF level (MeOH bulk); $\Delta E_{CORR(MP2,vacuo)}$ is the MP2 correction calculated in vacuo on the geometry optimized at the CASSCF level, and $\Delta G_{CORR(CASSCF,vacuo)}$ is the unscaled thermal correction to Gibbs free energy as from the output of the frequency calculation at the CASSCF level (in vacuo), also including the zero-point vibrational energy (ZPVE).

The level of theory chosen for optimizing aryl chlorides **1a**−**c** was CASSCF(10,10)/6-31G(d), with the 3π and 3π* orbitals of the aromatic ring and the σ/σ* couples of the C−Cl and C−Si bonds included in the active space. On the other hand, due to the huge memory requirement connected with their location, the active space was limited to the π system of the aromatic ring (comprising the 3π and the 3π* orbitals, resulting in a CASSCF(6,6) approach) when calculating the crossing point for **1a** (see Figure S4, Supporting Information, for details). Cations **2**$^+$**a**−**c** were optimized at the CASSCF(8,9)/6-31G(d), where the orbitals included in the active space were the 3π and the 3π* orbitals of the aromatic ring, the σ/σ* couple of the C−Si bond, and the orbital at the dicoordinated carbon (see Figure S5, Supporting Information, for details). DHTs **3a**−**c** were optimized at the CASSCF(8,8)/6-31G(d) level by including the 3π and the 3π* orbitals of the aromatic ring, the orbital at the benzylic position, and the orbital at the dicoordinated carbon in the active space (see Figure S6, Supporting Information, for details).

RESULTS

The present paper has been divided into four parts, corresponding to the key characteristics of the process, viz. (i) excitation and dechlorination of benzylsilanes **1a**-**c**, (ii) structure and properties of photogenerated phenyl cations **2**$^+$**a**−**c**, (iii) detachment of the TMS group from them, and (iv) relative stability of the α,n-DHTs (**3a**−**c**) obtained.

i. Excitation and Dechlorination of Benzylsilanes 1a−**c.** The heterolytic fragmentation of the C−Cl bond in the triplet state of electron-donating substituted phenyl halides has been documented by extended experimental studies. This found theoretical support from density functional theory (DFT) works.[1c−e,i] Early calculations carried out at the UB3LYP/6-311+G(2d,p) level had supported that heterolytic dehalogenation is a viable path in the lowest lying triplet state of derivatives **1a**−**c**.[6]

The present calculations at the CASSCF/6-31G(d) level showed that the lowest excited singlet state of (*n*-chlorobenzyl)trimethylsilanes (^{1}**1a**−**c**) lies ca. 100−110 kcal

dx.doi.org/10.1021/jo400269s | J. Org. Chem. 2013, 78, 3814−3820

mol^{-1} above the corresponding ground state (Scheme 2; Table S1, Supporting Information).

Scheme 2. Photochemistry of (*n*-Chlorobenzyl)-trimethylsilanes 1a−c

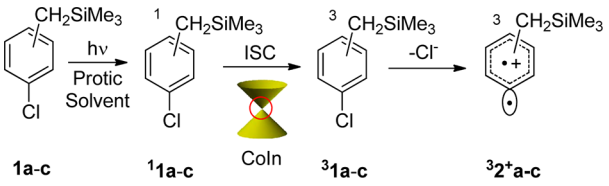

The optimized geometry of the *para*-isomer (^{1}**1a**) is reported in Figure 2b, along with some of the most relevant parameters.

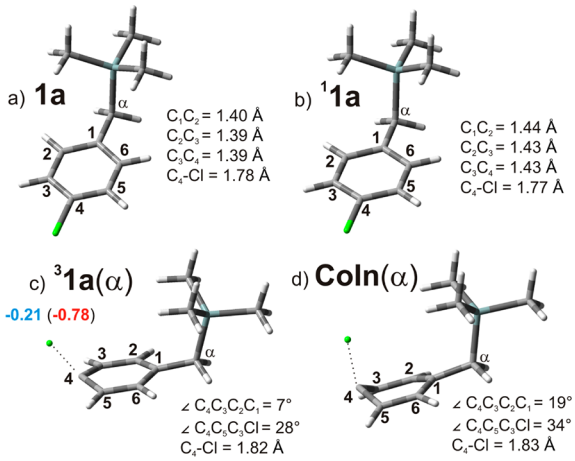

Figure 2. Optimized geometries at the CASSCF/6-31G(d) level and relevant parameters of (a) the ground state (**1a**), (b) the lowest excited singlet state (^{1}**1a**), and (c) the lowest triplet state (^{3}**1a**(α), absolute minimum) for compound **1a**. ESP charges (q_{ESP}) for the Cl atom at the equilibrium geometry and upon stretching of the C−Cl bond up to 2.6 Å are shown in blue and red, respectively, as derived from the results of calculations at the CPCM-CASSCF/6-31G(d) level of theory in bulk MeOH. (d) Optimized geometry at the CASSCF/6-31G(d) of the CoIn connecting the ^{1}**1a** and ^{3}**1a** (α, most stable structure) PESs, along with some of the most relevant parameters of this structure.

No distortion from the planarity occurs, and the aromatic ring somewhat expands with respect to **1a** (Figure 2a; see the different C−C bond lengths), while the C−Cl bond remains almost unchanged (only a minimal decrease, −0.01 Å; Figure 2b).

In contrast, the lowest triplet states (^{3}**1a−c**) are characterized by a marked distortion out of planarity of the ring. This originates two conformations, with the chlorine atom and the TMS group on the same side (hereafter tagged as geometry "α") or on opposite sides (geometry "β") with respect to the carbon skeleton. These are close in energy (ca. 66−68 kcal mol^{-1} above the corresponding ground state), with the α structure slightly more stable than the β in ^{3}**1a** (Figure 2c; Figure S1a and Table S1, Supporting Information), and the reverse situation with ^{3}**1b** and ^{3}**1c** (Figure S2 and Table S1, Supporting Information).[6]

Taking again compound **1a** as representative, it may be noticed that in the triplet state C_4 sticks out of the molecule plane (C_4−C_3−C_2−C_1 dihedral angle of 7°) and the C_4−Cl bond is further bent upward by an angle of 28° with respect to the C_4−C_5−C_3 plane and significantly elongated, from 1.78 to 1.82 Å. A negative charge develops at the chlorine atom (ca. −0.2; Figure 2c).

The potential energy curves reported in Figure 3 clearly show a different behavior when stretching the C−Cl bond with

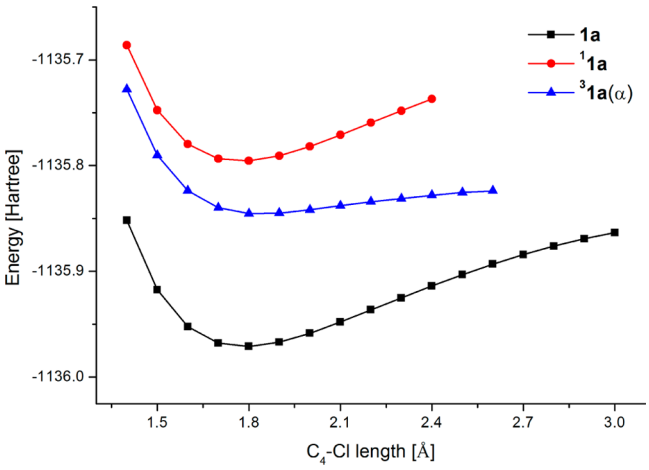

Figure 3. Potential energy curves for **1a**, ^{1}**1a**, and ^{3}**1a**(α) at the CPCM-CASSCF/6-31G(d) level of theory in bulk MeOH (see Table S2, Supporting Information, for details).

respect to the equilibrium geometry. Thus, in both the α and β geometries of ^{3}**1a**, stretching the C_4−Cl bond by ca. 1 Å with respect to the equilibrium geometry (final C_4−Cl bond length: 2.6 Å) involves a modest increase of energy (ca. 14 kcal mol^{-1} at the CPCM-CASSCF/6-31G(d) level of theory, Figure 3). Under these conditions, the chlorine atom acquires an almost full negative charge (ca. −0.8; see Figure 2c), supporting an easy loss of the chloride anion in the triplet state to afford the corresponding cation with the same multiplicity. On the contrary, stretching the C−Cl bond by only ca. 0.5 Å (final C_4−Cl bond length: 2.3 Å) in either the **1a** or the ^{1}**1a** states results in an energy increase of ca. 29 kcal mol^{-1} (Figure 3), with no significant negative charge localization at the chlorine atom.

As for the other two isomers, the investigation has been limited to the most stable triplet structure, viz. ^{3}**1b**(β) and ^{3}**1c**(β). Similar equilibrium geometries (Figure S2, Supporting Information) have been obtained for both isomers. In the case of ^{3}**1b**(β), the elongation of the C−Cl bond caused a charge redistribution similar to that of ^{3}**1a**(α) (Figure S2a, Supporting Information) and a comparable energy increase (ca. 16 kcal mol^{-1}). With ^{3}**1c**(β), however, the barrier was again ca. 16 kcal mol^{-1}, but the charge localization on the chlorine atom was only partial (ca. −0.4 at 2.6 Å C−Cl bond length, see Figure S2b, Supporting Information).

With the *para*-isomer **1a**, two different CoIns from ^{1}**1a** were located and these led to triplet ^{3}**1a**. These were again caused by the different orientation of the noncoplanar chlorine atom (α/β). The energies of these crossing points are close one to another, with the α conformer (Figure 2d) slightly more stable than the β one (Figure S1b, Supporting Information). The geometries of the two CoIns deserve some comment (Figure 2d). Thus, the C_4 atom is bent out of the aromatic plane and the C−Cl bond lies almost perpendicularly with respect to the carbon skeleton and is markedly elongated. These features prefigure those of the triplet state and, indeed, are even more pronounced.

dx.doi.org/10.1021/jo400269s | J. Org. Chem. 2013, 78, 3814−3820

ii. Structure and Properties of Photogenerated Phenyl Cations 2⁺a–c. *Triplet Phenyl Cations.* Triplet phenyl cations (^{3}**2⁺a–c**) are perfectly planar and minimally differ from the original benzene geometry. The CASSCF results show that the reference configuration accounts for more than 85% to the overall wave function, and the coefficient of the lowest eigenvector is >0.93 in every case. The occupancies of the orbitals included in the active space are close to 2, 1, and 0, and the localization of the two unpaired electrons is easily determined. Thus, one of the singly occupied orbitals is located at the dicoordinated carbon, while the other is part of the π system, as seen for the two singly occupied orbitals of ^{3}**2⁺a** in Figure 4 (similar results for the other isomers).

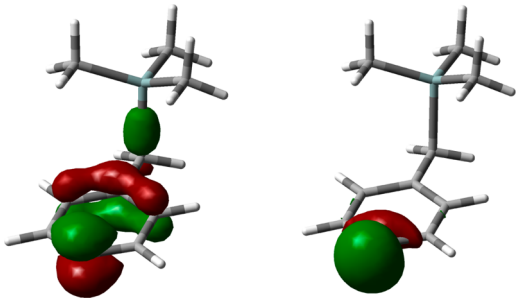

Figure 4. Singly occupied orbitals for ^{3}**2⁺a**, as determined from CPCM-CASSCF/6-31G(d) calculations in bulk MeOH.

These intermediates thus resemble phenyl radicals on one hand and benzene radical cations on the other one. Because of this structure, in all of the isomeric cations ^{3}**2⁺** the positive charge is mainly delocalized on the aromatic ring and only a fraction resides at the dicoordinated carbon atom (q_{ESP} < 0.1 as from CPCM-CASSCF/6-31G(d) calculations in MeOH bulk).

Singlet Phenyl Cations. All of the singlet phenyl cations ^{1}**2⁺a–c** deviate from the planar, regular hexagonal structure. Both in the *ortho*- and *para*-isomers, the dicoordinated carbon is shifted out of the plane, while in the *meta*-isomer this is in the plane and the deformation involves the two adjacent carbon atoms (in particular, the C atom in the *para*-position with respect to the substituent). In any case, the lack of planarity leads to a mixing of the orbital at the dicoordinated carbon and the aromatic system. A detailed analysis of the orbitals included in the active space highlights that the mixing involves one of the doubly occupied π orbitals and the σ orbital.

As an example, Figure 5 shows the shape of the two resulting orbitals (tagged as Φ_A and Φ_B) for the case of ^{1}**2⁺b**, which differs little from that of isomers ^{1}**2⁺a** and ^{1}**2⁺c**. In all of ^{1}**2⁺**, the configuration with the highest eigenvector has 2 and 0 electrons in Φ_A and Φ_B, respectively, and the second most important one is doubly excited, with 0 and 2 electrons in Φ_A and Φ_B, respectively (see Figure 5 for a schematic representation for ^{1}**2⁺b**). However, the electronic structure of both ^{1}**2⁺a** and ^{1}**2⁺c** can be described with good approximation by using only the reference determinant ($\Phi_A^2\Phi_B^0$; the coefficient of this configuration is ca. 0.92 in both cases), while the second configuration contributes more significantly in the case of ^{1}**2⁺b** (see Table 1). This situation is reflected in the occupancies of Φ_A and Φ_B, where a significant displacement of electrons from the former to the latter is apparent only in the *meta*-isomer, while it is negligible in both the *ortho*- and *para*-analogues. As a result, the charge at the discoordinated carbon is almost one-half for ^{1}**2⁺b** with respect to both ^{1}**2⁺a** and ^{1}**2⁺c** (Table 1).

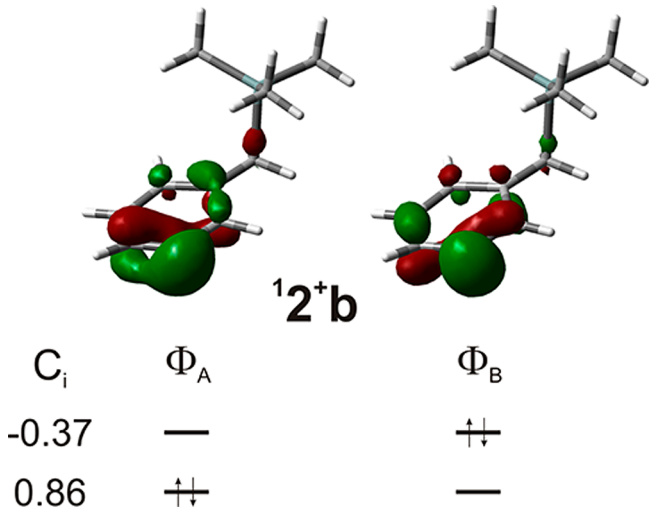

Figure 5. Schematic depiction of the electronic structure of ^{1}**2⁺b** as from calculations at the CPCM-CASSCF/6-31G(d) level of theory in bulk MeOH. The coefficients (C_i) of the two main electronic configurations (viz. $\Phi_A^2\Phi_B^0$ and $\Phi_A^0\Phi_B^2$, see also Table 1 for details) for this species are reported.

Table 1. Selected Data for the Three Isomeric Singlet Phenyl Cations (^{1}2⁺) as from Calculations at the CPCM-CASSCF/6-31G(d) Level of Theory in MeOH Bulk

	configuration coefficients		orbital occupancies		
cations	$\Phi_A^2\Phi_B^0$	$\Phi_A^0\Phi_B^2$	Φ_A	Φ_B	ESP charge at dicoordinated C
^{1}**2⁺a**	0.922	−0.188	1.85	0.14	0.224
^{1}**2⁺b**	0.856	−0.372	1.64	0.37	0.136
^{1}**2⁺c**	0.937	−0.120	1.87	0.12	0.259

Relative Energy of Phenyl Cations. The isodesmic reaction reported in eq 2 was used to quantify the stabilization of the isomeric phenyl cations **2⁺a-c** by the $-CH_2TMS$ substituent with respect to the parent singlet phenyl cation taken as the reference.

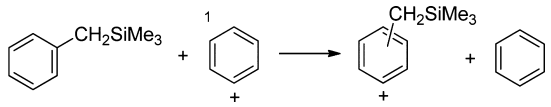

(2)

The results are graphically shown in Figure 6 (see also Table S4, Supporting Information), where the relative energies of the six isomeric phenyl cations are reported, as obtained from eq 2. Thus, all of the cations considered here are less stable than ^{1}Ph⁺. As previously observed for other substituted phenyl cations,[1e] the energy order of the states of either multiplicity depends on the position of the substituent. Thus, the ground state of **2⁺a** is a triplet, and those of **2⁺b** and **2⁺c** are singlets.

iii. Detachment of TMS Group from Phenyl Cations 2⁺a–c. The key step allowing for the formation of DHTs is the loss of the TMS cation at the phenyl cation stage. This process has been simulated by computational means by having recourse to a relaxed PES scan, viz. by stretching the C_α–Si bond in **2⁺a–c** from the equilibrium geometry up to 3.5 Å by 0.1 Å intervals (see the Supporting Information for details). This leads, as expected, to the expulsion of the TMS cation and

dx.doi.org/10.1021/jo400269s | J. Org. Chem. 2013, 78, 3814–3820

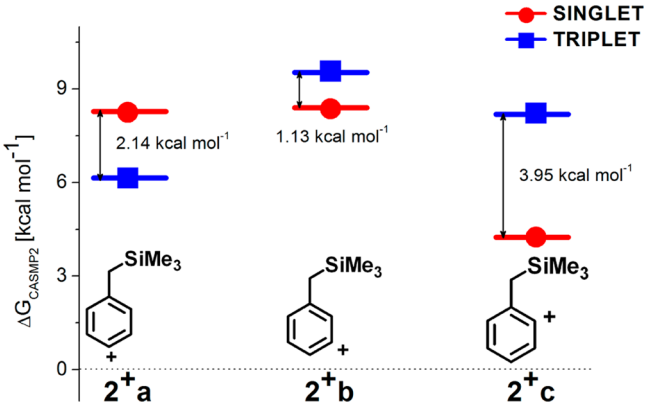

Figure 6. Relative energies of phenyl cations $\mathbf{2}^+\mathbf{a}-\mathbf{c}$ according to the isodesmic reaction in eq 2.

shows that the charge associated to this group is ca. +0.93 when $C_\alpha-Si \sim 3.5$ Å with all of the isomers.

Figure 7a–c shows the energy profiles (expressed as total electronic energy at the CPCM–CASSCF/6-31G(d) level of theory, that is by plotting the $E_{0(CASSCF,CPCM)}$ values; see also Table S7, Supporting Information) for $\mathbf{2}^+\mathbf{a}-\mathbf{c}$ upon elongation of the C_α–Si bond. The energy gaps at the equilibrium geometry for $\mathbf{2}^+\mathbf{a}-\mathbf{c}$ reported in Figure 6 differ from those in Figure 7a–c, since the level of theory is different ($E_{0(CASSCF,CPCM)}$ vs G_{CASMP2}). We deemed appropriate evaluating the energy variation involved in the detachment of the TMS by referring to the total electronic energy in solvent (MeOH), without including any of the correction terms reported in eq 1, since the structures plotted are not stationary points on the PESs, apart from the first point on the left in each series (that refers to the equilibrium geometry of $\mathbf{2}^+\mathbf{a}-\mathbf{c}$). In all cases, no transition state was observed and the energy increased monotonically with the stretching of the C_α–Si bond. There was a difference, however, between the *ortho*- and *para*-singlets ($^1\mathbf{2}^+\mathbf{a}$ and $^1\mathbf{2}^+\mathbf{c}$), characterized by a short C_α–Si bond length at the equilibrium geometry (1.95–2.00 Å) on one hand and the *meta*-singlet and the triplets (2.05–2.10 Å) on the other one. The barrier is higher for the two first intermediates (23–27 kcal mol^{-1}) with a sharp increase at the beginning (from ca. 2.0 to 2.4 Å), while a lower barrier (18–20 kcal mol^{-1}) is encountered with the other four species, where a smooth profile is followed. This corresponds to a clear-cut geometric variation with $^1\mathbf{2}^+\mathbf{a}$ and $^1\mathbf{2}^+\mathbf{c}$, where the initially puckered ring tends to planarize at the beginning of the process simultaneously with the incipient removal of the TMS group and the formation of the second radical site at the benzylic position. This feature is not present for the case of triplets $^3\mathbf{2}^+\mathbf{a}-\mathbf{c}$ (perfectly planar) and of $^1\mathbf{2}^+\mathbf{b}$ (small deviation from planarity). For the sake of comparison

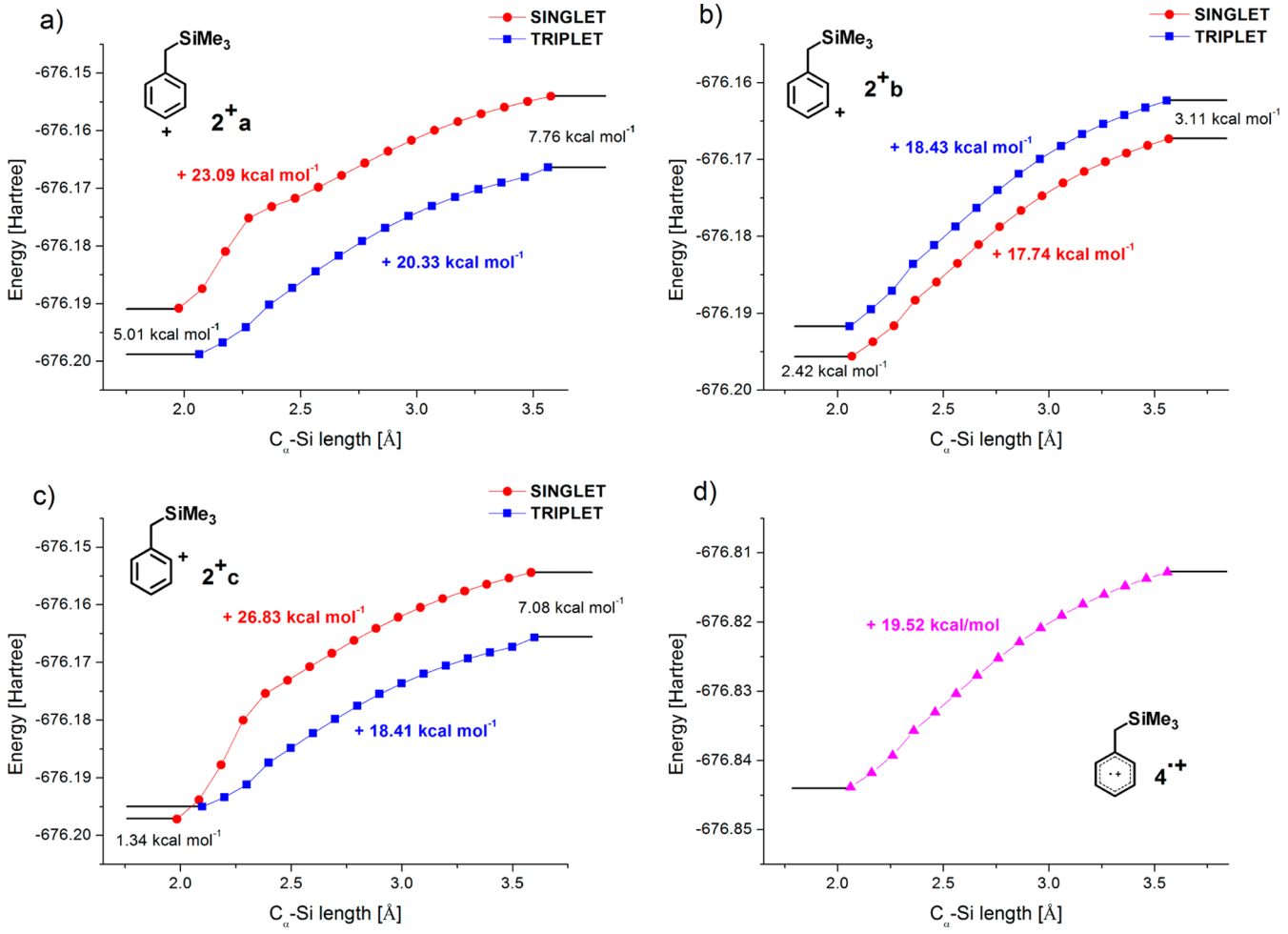

Figure 7. Energy profiles for the relaxed scans of the C_α-Si bond in (a) $\mathbf{2}^+\mathbf{a}$, (b) $\mathbf{2}^+\mathbf{b}$, (c) $\mathbf{2}^+\mathbf{c}$, (d) $\mathbf{4}^{\bullet+}$ at the CPCM-CASSCF/6-31G(d) level of theory in bulk MeOH.

dx.doi.org/10.1021/jo400269s | J. Org. Chem. 2013, 78, 3814–3820

(see Discussion), the elimination of the TMS cation from benzyltrimethylsilane radical cation ($4^{\bullet+}$) was calculated by the same approach and gave a result similar to those of the second family (Figure 7d; see Table S8, Supporting Information, for details).

iv. Relative stability of α,*n*-DHTs 3a−c. The energy of these intermediates has been previously determined[20] and was now calculated with the above computational approach for the sake of completeness. In accordance with the literature, the ground state of the *ortho*- and *para*-isomers was found to be a triplet (ca. 6 kcal mol^{-1} gap), whereas the singlet and the triplet lie closer in the *meta*-isomer, with the former slightly more stable than the latter (see Tables S5−S6 and Figure S3, Supporting Information, for details).[20]

DISCUSSION

The above-reported computational data along with the product distribution observed in the photolysis of **1a−c**[6] support the photogeneration of α,*n*-DHTs (**3a−c**) from **1a−c** via cations $\mathbf{2}^{+}$**a−c**. In turn, the last intermediates resulted from the heterolytic fragmentation of the aryl−chlorine bond in the triplet states ^{3}**1a−c** in a polar medium, as fully supported by computational means. These states are experimentally known to be efficiently populated in electron-rich aromatic halides (with a rate constant $k_{ISC} > 10^{9}$ s^{-1}).[21] The present work localizes the CoIns allowing this process to occur. The effect of the trimethylsilyl group on the photophysics of compounds **1a−c** is expected to be marginal since benzylsilane has the same fluorescence (Φ_f) and phosphorescence (Φ_p) quantum yield of toluene[22] and the Φ_f of **1a** is comparable to that of 4-chlorotoluene.[6,23]

The calculations clearly evidence that the singlets show no deformation in the direction of C−Cl cleavage. On the contrary, in the triplets this bond sticks out from the molecule plane and a negative charge develops at the chlorine atom. An almost full negative charge was observed when stretching the Ar−Cl bond by ca. 1 Å with respect to the equilibrium geometry in ^{3}**1a,b**. Charge separation, however, is less significant in the case of ^{3}**1c**, which exhibits the lowest photoreactivity in the series.[6] Thus, heterolysis occurring in ^{3}**1a−c** gives phenyl cations in the same multiplicity ($^{3}\mathbf{2}^{+}$**a−c**).

The path leading to triplet α,*n*-DHTs (^{3}**3a−c**, path *a*) is shown in Scheme 3 along with alternative paths, viz. reduction (path *b*) and ISC to the singlet phenyl cation ($^{1}\mathbf{2}^{+}$**a-c**, path *c*). The last intermediate may in turn undergo solvolysis (path *d*) or desilylation to give singlet DHT (^{1}**3a−c**, path *a′*), accessible also by ISC from the corresponding triplets (path *c′*). When a selective trap of triplet phenyl cations is present, e.g., allyltrimethylsilane, arylation can likewise take place (path *e*).

In the case of $^{3}\mathbf{2}^{+}$**b** and $^{3}\mathbf{2}^{+}$**c**, ISC to the more stable (by 1.1 and almost 4 kcal mol^{-1}, respectively) singlet phenyl cations $^{1}\mathbf{2}^{+}$**b,c** is feasible (Figure 5), but solvolysis products (path *d*), which are diagnostic of the role of singlet cations, were not detected. On the other hand, calculations showed that cation $^{1}\mathbf{2}^{+}$**c** confronts the highest barrier for TMS^{+} loss (+26.83 kcal mol^{-1}, Figure 6c), while both spin states of the *meta*-cation $\mathbf{2}^{+}$**b** desilylate over a comparable energy (+17.74 and +18.43 kcal mol^{-1}, respectively, Figure 6b). Accordingly, cation $^{1}\mathbf{2}^{+}$**c** has no role here and we can safely conclude that the *ortho*- and *para*-DHTs can be exclusively generated in their triplet ground states (see Figure S3, Supporting Information) from the corresponding triplet cations via path *a*. The different products distribution

Scheme 3. Accessible Paths from Triplet Phenyl Cations $^{3}\mathbf{2}^{+}$a−c

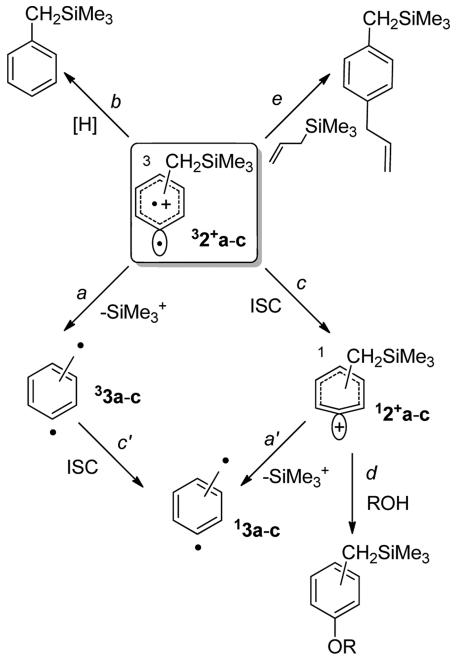

("radical" vs "ionic" products)[6,7,24] experimentally observed in the α,3-DHT points to the involvement of a different intermediate. At the present stage, we surmise that ground state ^{1}**3b** could be a valid candidate. Actually, the latter species can be generated from $^{3}\mathbf{2}^{+}$**b** both via path *a* → *c′* and via ISC then cleavage (path *c* → *a′*). Neither of the two pathways can be safely excluded. The interconversion between different spin states of (substituted) phenyl cations is supported by DFT calculations,[1b,25] and is claimed to be rapid for states close in energy.[1b] However, at the best of our knowledge, no information is available for the same process in the case of DHTs.

CONCLUSIONS

The present work demonstrates that the multireference approach CASSCF allows to rationalize the photogeneration and the relative stability of phenyl cations as well as the generation of DHTs by loss of TMS^{+} from the benzylic position. The latter reaction occurs when the charge is delocalized over the aromatic ring, as typical of triplet states, but also for a charge-delocalized singlet such as $^{1}\mathbf{2}^{+}$**b**. This computational study encourages to pursue the exploration of this entry to such important intermediates as DHTs and evidences how obtaining a picture of the electronic structure may widen the understanding of the chemistry of such little known intermediates. In particular, new facets of the chemistry of phenyl cations, intermediates of perhaps unsuspected versatility, have been revealed.

ASSOCIATED CONTENT

Supporting Information

Optimized geometries, energies, and CASSCF output data for all structures involved in this work. This material is available free of charge via the Internet at http://pubs.acs.org.

dx.doi.org/10.1021/jo400269s | J. Org. Chem. 2013, 78, 3814−3820

AUTHOR INFORMATION

Corresponding Author

*Tel: +39 0382 987316. Fax: +39 0382 987323. E-mail: fagnoni@unipv.it.

Notes

The authors declare no competing financial interest.

ACKNOWLEDGMENTS

S.P. acknowledges MIUR, Rome (FIRB-Futuro in Ricerca 2008 project RBFR08J78Q), for financial support. This work has been supported by the Fondazione Cariplo (Grant No. 2011-1839). This work was funded by the CINECA Supercomputer Center, with computer time granted by the ISCRA COMPDHT (HP10CZEHG6) project. We thank Professors P. Caramella and R. Gandolfi of the University of Pavia for helpful discussions and Professor A. Bagno of the University of Padova for support.

REFERENCES

(1) (a) Nicolaides, A.; Smith, D. M.; Jensen, F.; Radom, L. *J. Am. Chem. Soc.* **1997**, *119*, 8083−8088. (b) Aschi, M.; Harvey, J. N. *J. Chem. Soc., Perkin Trans. 2* **1999**, 1059−1062. (c) Freccero, M.; Fagnoni, A.; Albini, A. *J. Am. Chem. Soc.* **2003**, *125*, 13182−13190. (d) Dichiarante, V.; Salvaneschi, A.; Protti, S.; Dondi, D.; Fagnoni, M.; Albini, A. *J. Am. Chem. Soc.* **2007**, *129*, 15919−15926. (e) Dichiarante, V.; Dondi, D.; Protti, S.; Fagnoni, M.; Albini, A. *J. Am. Chem. Soc.* **2007**, *129*, 5605−5611; **2007**, *129*, 11662 (correction). (f) Lazzaroni, S.; Dondi, D.; Fagnoni, M.; Albini, A. *J. Org. Chem.* **2008**, *73*, 206−211. (g) Lazzaroni, S.; Dondi, D.; Fagnoni, M.; Albini, A. *J. Org. Chem.* **2010**, *75*, 315−323. (h) Bondarchuk, S. V.; Minaev, B. F. *Chem. Phys.* **2011**, *389*, 68−74. (i) Raviola, C.; Protti, S.; Ravelli, D.; Mella, M.; Albini, A.; Fagnoni, M. *J. Org. Chem.* **2012**, *77*, 9094−9101. (j) Gasper, S. M.; Devadoss, C.; Schuster, G. B. *J. Am. Chem. Soc.* **1995**, *117*, 5206−5211.

(2) Fagnoni, M.; Albini, A. *Acc. Chem. Res.* **2005**, *38*, 713−721.

(3) Dichiarante, V.; Fagnoni, M. *Synlett* **2008**, 787−800 and references cited therein.

(4) See, for instance: Stang, P. J. In *Dicoordinated Carbocations*; Rappoport, Z., Stang, P. J., Eds.; Wiley: New York, 1997; pp 451−460. Subramanian, L. R.; Hanack, M.; Chang, L. W. K.; Imhoff, M. A.; Schleyer, P. v. R.; Effenberger, F.; Kurtz, W.; Stang, P. J.; Dueber, T. E. *J. Org. Chem.* **1976**, *41*, 4099−4103. Himeshima, Y.; Kobayashi, H.; Sonoda, T. *J. Am. Chem. Soc.* **1985**, *107*, 5286−5288. Apeloig, Y.; Arad, D. *J. Am. Chem. Soc.* **1985**, *107*, 5285−5286.

(5) Protti, S.; Dondi, M.; Mella, M.; Fagnoni, M.; Albini, A. *Eur. J. Org. Chem.* **2011**, 3229−3237. Manet, I.; Monti, S.; Grabner, G.; Protti, S.; Dondi, D.; Dichiarante, V.; Fagnoni, M.; Albini, A. *Chem.—Eur. J.* **2008**, *14*, 1029−1039. Protti, S.; Dichiarante, V.; Dondi, D.; Fagnoni, M.; Albini, A. *Chem. Sci.* **2012**, *3*, 1330−1337.

(6) Protti, S.; Ravelli, D.; Mannucci, B.; Albini, A.; Fagnoni, M. *Angew. Chem., Int. Ed.* **2012**, *51*, 8577−8580.

(7) (a) Myers, A. G.; Parrish, C. A. *Bioconjugate Chem.* **1996**, *7*, 322−331. (b) Kuzmin, A. V.; Popik, V. V. *Chem. Commun.* **2009**, 5707−5709.

(8) See, for reviews: (a) Wang, K. K. *Chem. Rev.* **1996**, *96*, 207−222. (b) Myers, A. G.; Kuo, E. Y.; Finney, N. S. *J. Am. Chem. Soc.* **1989**, *111*, 8057−8059. (c) Alabugin, I. V.; Yang, W.-Y.; Pal, R. In *CRC Handbook of Organic Photochemistry and Photobiology*, 3rd ed.; Griesbeck, A., Oelgemoeller, M., Ghetti, F., Eds.; CRC Press: Boca Raton, 2012; pp 549−592. (d) Breiner, B.; Kaya, K.; Roy, S.; Yang, W.-Y.; Alabugin, I. V. *Org. Biomol. Chem.* **2012**, *10*, 3974−3987. (e) Kar, M.; Basak, A. *Chem. Rev.* **2007**, *107*, 2861−2890 and references therein.

(9) Alternative approaches proposed for the generation of α,n-DHT isomers are not suitable for preparative application; see for instance: Wenthold, P. G.; Wiershke, S. G.; Nash, J. J.; Squires, R. R. *J. Am. Chem. Soc.* **1994**, *116*, 7378−7392. Neuhaus, P.; Henkel, S.; Sander, W. *Aust. J. Chem.* **2010**, *63*, 1634−1637. Wiersum, U. E.; Nieuwenhuis, T. *Tetrahedron Lett.* **1973**, *14*, 2581−2584.

(10) Hansch, C.; Leo, A.; Taft, R. W. *Chem. Rev.* **1991**, *91*, 165−195.

(11) Dinnocenzo, J. P.; Farid, S.; Goodman, J. L.; Gould, I. R.; Mattes, S. L.; Todd, W. P. *J. Am. Chem. Soc.* **1989**, *111*, 8973−8975.

(12) Mella, M.; Coppo, P.; Guizzardi, B.; Fagnoni, M.; Freccero, M.; Albini, A. *J. Org. Chem.* **2001**, *66*, 6344−6352.

(13) Bachrach, S. M. Diradicals and Carbenes. In *Computational Organic Chemistry*; John Wiley & Sons: Hoboken, 2006.

(14) Roos, B. O. *Int. J. Quantum Chem. Symp.* **1980**, *14*, 175−189.

(15) Møller, C.; Plesset, M. S. *Phys. Rev.* **1934**, *46*, 618−622.

(16) Gaussian 03, Revision D.01: Frisch, M. J.; Trucks, G. W.; Schlegel, H. B.; Scuseria, G. E.; Robb, M. A.; Cheeseman, J. R.; Montgomery, J. A., Jr.; Vreven, T.; Kudin, K. N.; Burant, J. C.; Millam, J. M.; Iyengar, S. S.; Tomasi, J.; Barone, V.; Mennucci, B.; Cossi, M.; Scalmani, G.; Rega, N. Petersson, G. A.; Nakatsuji, H.; Hada, M.; Ehara, M.; Toyota, K.; Fukuda, R.; Hasegawa, J.; Ishida, M.; Nakajima, T.; Honda, Y.; Kitao, O.; Nakai, H.; Klene, M.; Li, X.; Knox, J. E.; Hratchian, H. P.; Cross, J. B.; Adamo, C.; Jaramillo, J.; Gomperts, R.; Stratmann, R. E.; Yazyev, O.; Austin, A. J.; Cammi, R.; Pomelli, C.; Ochterski, J. W.; Ayala, P. Y.; Morokuma, K.; Voth, G. A.; Salvador, P.; Dannenberg, J. J.; Zakrzewski, V. G.; Dapprich, S.; Daniels, A. D.; Strain, M. C.; Farkas, O.; Malick, D. K.; Rabuck, A. D.; Raghavachari, K.; Foresman, J. B.; Ortiz, J. V.; Cui, Q.; Baboul, A. G.; Clifford, S.; Cioslowski, J.; Stefanov, B. B.; Liu, G.; Liashenko, A.; Piskorz, P.; Komaromi, I.; Martin, R. L.; Fox, D. J.; Keith, T.; Al-Laham, M. A.; Peng, C. Y.; Nanayakkara, A.; Challacombe, M.; Gill, P. M. W.; Johnson, B.; Chen, W.; Wong, M. W.; Gonzalez, C.; Pople, J. A. Gaussian, Inc., Pittsburgh PA, 2003.

(17) (a) Yarkony, D. R. *Acc. Chem. Res.* **1998**, *31*, 511−518. (b) Yarkony, D. R. *Rev. Mod. Phys.* **1996**, *68*, 985−1013. (c) Bernardi, F.; Olivucci, M.; Robb, M. A. *Chem. Soc. Rev.* **1996**, *25*, 321−328. (d) Bernardi, F.; Olivucci, M.; Robb, M. A. *Pure Appl. Chem.* **1995**, *67*, 17−24. (e) Yarkony, D. R. *J. Phys. Chem.* **1993**, *97*, 4407−4412.

(18) Barone, V.; Cossi, M. *J. Phys. Chem. A* **1998**, *102*, 1995−2001.

(19) Besler, B. H.; Merz, K. M., Jr.; Kollman, P. A. *J. Comput. Chem.* **1990**, *11*, 431−439. Singh, U. C.; Kollman, P. A. *J. Comput. Chem.* **1984**, *5*, 129−145.

(20) Cabrero, J.; Ben-Amor, N.; Caballol, R. *J. Phys. Chem. A* **1999**, *103*, 6220−6224.

(21) (a) Previtali, C. M.; Ebbesen, T. W. *J. Photochem.* **1985**, *30*, 259−267. (b) Han, K.-L.; He, G.-Z. *J. Photochem. Photobiol. C* **2007**, *8*, 55−66. (c) Koutek, B.; Musil, L.; Velek, J.; Souček, M. *Collect. Czech. Chem. Commun.* **1985**, *50*, 1753−1763. (d) Gu, X.-B.; Wang, G.-J.; Huang, J.-H.; Han, K.-L.; He, G.-Z.; Lou, N.-Q. *Phys. Chem. Chem. Phys.* **2002**, *4*, 6027−6033.

(22) Hiratsuka, H.; Kobayashi, S.; Minegishi, T.; Hara, M.; Okutsu, T.; Murakami, S. *J. Phys. Chem. A* **1999**, *103*, 9174−9183.

(23) Nijegorodov, N.; Mabbs, R. *Spectrochim. Acta A* **2001**, *57*, 1449−1462.

(24) Myers, A. G.; Dragovich, P. S.; Kuo, E. Y. *J. Am. Chem. Soc.* **1992**, *114*, 9369−9386. Cremeens, M. E.; Hughes, T. S.; Carpenter, B. K. *J. Am. Chem. Soc.* **2005**, *127*, 6652−6661.

(25) (a) Bondarchuk, S. V.; Minaev, B. F. *THEOCHEM* **2010**, *952*, 1−7. (b) Harvey, J. N.; Aschi, M.; Schwarz, H.; Koch, W. *Theor. Chem. Acc.* **1998**, *99*, 95−99.